Neuron
Article

Widespread Receptivity to Neuropeptide PDF throughout the Neuronal Circadian Clock Network of *Drosophila* Revealed by Real-Time Cyclic AMP Imaging

Orie T. Shafer,[1] Dong Jo Kim,[1] Richard Dunbar-Yaffe,[3] Viacheslav O. Nikolaev,[2] Martin J. Lohse,[2] and Paul H. Taghert[1,*]
[1]Department of Anatomy & Neurobiology, Washington University School of Medicine, 660 S. Euclid Avenue, St. Louis, MO 63110, USA
[2]Institute of Pharmacology and Toxicology, University of Würzburg, Verbacherstrasse 9, D-97078, Würzburg, Germany
[3]Department of Biology, University of Toronto at Mississauga, Mississauga, ON L5L 1C6, Canada
*Correspondence: taghertp@pcg.wustl.edu
DOI 10.1016/j.neuron.2008.02.018

SUMMARY

The neuropeptide PDF is released by sixteen clock neurons in *Drosophila* and helps maintain circadian activity rhythms by coordinating a network of ~150 neuronal clocks. Whether PDF acts directly on elements of this neural network remains unknown. We address this question by adapting Epac1-camps, a genetically encoded cAMP FRET sensor, for use in the living brain. We find that a subset of the PDF-expressing neurons respond to PDF with long-lasting cAMP increases and confirm that such responses require the PDF receptor. In contrast, an unrelated *Drosophila* neuropeptide, DH31, stimulates large cAMP increases in all PDF-expressing clock neurons. Thus, the network of ~150 clock neurons displays widespread, though not uniform, PDF receptivity. This work introduces a sensitive means of measuring cAMP changes in a living brain with subcellular resolution. Specifically, it experimentally confirms the longstanding hypothesis that PDF is a direct modulator of most neurons in the *Drosophila* clock network.

INTRODUCTION

The molecular clock is expressed throughout the body of the fly *Drosophila* but is required in only a subset of the approximately 150 central clock-expressing neurons for the maintenance of locomotor rhythms (Figure 1A; reviewed by Taghert and Shafer, 2006). For example, the lateral neurons (LNs)—comprising the ventrolateral and dorsolateral neurons—are required for normal locomotor rhythms (Helfrich-Förster, 1998). Sixteen LNs, the eight large and eight small ventrolateral neurons (the l-vLNs and s-vLNs,) express pigment dispersing factor (PDF) (Helfrich-Förster, 1995), a neuropeptide required for normal circadian control of locomotion under constant darkness and temperature (DD) and for morning activity under light:dark (LD) conditions (Renn et al., 1999). The remaining LNs, the fifth s-vLN, and the dorsal lateral neurons (dLNs), do not express PDF and have been implicated in the control of evening activity under LD (Stoleru et al., 2004; Grima et al., 2004; Rieger et al., 2006). Here, we regard all circadian clock-expressing neurons in the *Drosophila* brain to be circadian pacemakers.

PDF-expressing s-vLNs are the dominant circadian pacemakers under LD and DD conditions. (e.g., Renn et al., 1999; Stoleru et al., 2005; Rieger et al., 2006; Picot et al., 2007). Genetic loss of PDF results in similar changes as found with ablation of vLNs: modification of entrained rhythms and weakening of free-running rhythms (Renn et al., 1999; Blanchardon et al., 2001), suggesting the release of PDF from these cells is a critical component of the neuronal clock network. Furthermore, PDF is necessary for normal clock synchronization and phase adjustment (Peng et al., 2003; Lin et al., 2004). Several reports identified a G protein-coupled-receptor (GPCR) for PDF, referred to here as PDFr (Hyun et al., 2005; Lear et al., 2005; Mertens et al., 2005), but have not produced a consistent picture of where PDFr is expressed. Given the importance of PDF for the maintenance of circadian rhythms, the identification of its targets and determination of its signaling mechanisms represent significant goals to understand the clock network in the fly.

Recently, genetically encoded Ca^{2+} sensors have been introduced to help map connectivity and receptivity in the central nervous system (CNS) of the fly (e.g., Wang et al., 2003; Suh et al., 2004). These efforts suggest that real-time imaging could likewise be used to map PDF receptivity. PDFr belongs to the family B (secretin receptor) group of receptors and is most closely related to the calcitonin-CGRP receptors (Hewes and Taghert, 2001). In vitro, it signals predominantly through cAMP and only weakly through Ca^{2+} (Hyun et al., 2005; Mertens et al., 2005). Therefore, the technical advantages offered by dyes and genetically encoded sensors for Ca^{2+} will likely not suffice to elucidate fundamental details of PDF signaling in vivo.

To address this issue, we turned to methods of real-time cAMP measures that harness the cAMP-binding properties of Epac (exchange protein directly activated by cAMP)—a molecule mediating non-protein kinase A (PKA)-dependent cAMP signaling (de Rooij et al., 1998). Epac is a cAMP-activated guanine nucleotide exchange factor for Rap1 (Bos, 2003) and has clear advantages over PKA as the basis for a cAMP reporter system because it binds cAMP as a monomer and displays more rapid activation and relaxation kinetics (DiPilato et al., 2004; Nikolaev et al., 2004; Ponsioen et al., 2004). In two Epac-based sensors (DiPilato et al., 2004; Ponsioen et al., 2004) a full-length Epac protein is flanked by cyan fluorescent protein (CFP) and by yellow fluorescent protein (YFP). In a second class of Epac-based

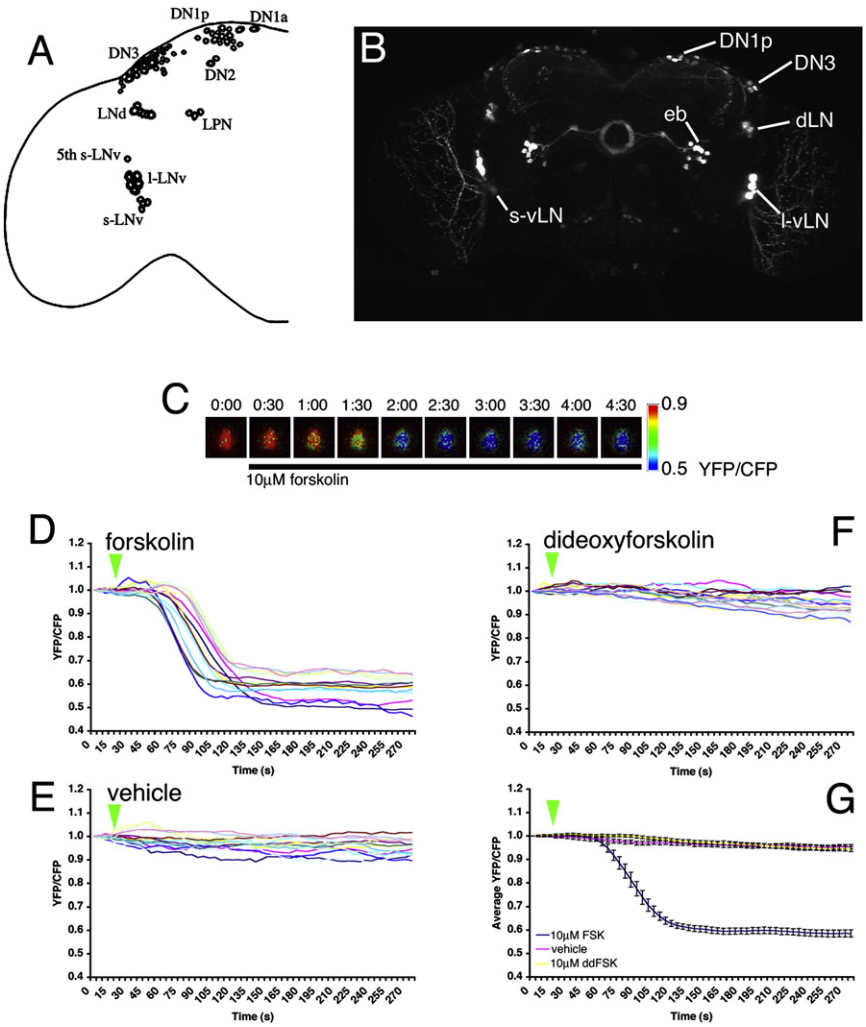

Figure 1. Epac1-camps Is Stably Expressed in the Neuronal Circadian Clock Network and Retains Its Function as a cAMP Reporter

(A) Schematic representation of nine classes of circadian clock neurons in a single hemisphere of the adult brain.

(B) Anterior aspect confocal Z series of YFP emission in a *uas-Epac1-camps(42A);Cry(39)-Gal4* brain. Visible neuronal clock classes are labeled, as are neurons of the ellipsoid body (eb).

(C) A pseudocolored time course of Epac1-camps FRET loss in a single l-vLN cell body in response to 10 μM FSK. The black bar beneath the panels indicates the presence of FSK. The look-up table values represent unnormalized YFP/CFP ratios.

(D) The responses of 14 l-vLNs from five brains to 10 μM FSK. In all graphs the green triangles indicate the start of bath application.

(E) The responses of 14 l-vLNs from five brains to vehicle (0.1% DMSO in HL3 saline).

(F) The responses of 15 l-vLNs from five brains to 10 μM ddFSK, a biologically inactive form of FSK.

(G) Summary plots of the data in (D)–(F) displaying the average YFP/CFP value for each time point. In this and all other figures, error bars indicate the standard error of the mean (SEM). Data were analyzed through one-way repeated-measures ANOVA with fixed factor drug (vehicle, FSK, ddFSK) and within-subjects factor time. The ANOVA revealed a significant within-subjects effect of time on the measurement of the normalized ratio ($p < 0.001$), and a significant effect of the drug used on the ratio recorded ($p < 0.001$). Finally, FSK, vehicle, and ddFSK can be broken into two homogenous subsets: FSK and vehicle/ddFSK, which are homogenous statistically.

sensor, CFP and YFP flank a truncated Epac1, containing only the cAMP-binding domain, thus decreasing the likelihood of interference with cellular functions (Nikolaev and Lohse, 2006). We have employed this second class—specifically Epac1-camps (Nikolaev et al., 2004)—for use in living fly brain. When not bound to cAMP, the Epac-based sensors support fluorescence resonance energy transfer (FRET) from CFP to YFP. The binding of cAMP forces the CFP and YFP domains to move apart leading to a reduction in FRET levels when cAMP levels rise.

Our work with Epac1-camps in the circadian clock network of *Drosophila* indicates that this sensor is sensitive and suitable for the detection of GPCR-induced cAMP signaling in the living fly brain. We use it here to address the important hypothesis, widely held but not previously tested, that PDF is a direct modulator of the neurons within the *Drosophila* clock network.

RESULTS

Fly Neurons Tolerate Epac1-camps Expression

As a first step toward the live imaging of cAMP dynamics in fly neurons, we evaluated the degree to which expression of the FRET reporter Epac1-camps affected *Drosophila* neuronal morphology and behavior. We crossed several *uas-Epac1-camps* lines to a suite of Gal4 drivers whose expression patterns have been described (Figure 1B and see Figures S1A–S1D available online). Among the progeny of these crosses, we found no indication of developmental abnormalities or delays and likewise found no evidence of neuronal abnormality. Typically, Epac1-camps fluorescence was found in both the soma and projections of neurons. For example, crossing *uas-Epac1-camps* to *Cry(39)-Gal4* yielded brains in which Epac1-camps CFP and YFP could be detected within the soma and projections of all classes of clock neuron except the lateral posterior neurons (Figure 1B). *Cry(39)-Gal4* also drove Epac1-camps expression in the ellipsoid body neurons of the central complex (Figure 1B).

To determine if the expression of the FRET reporter may have produced a cryptic disruption in neurons, we assayed the daily locomotor behavior of *Pdf(M)-Gal4/y;uas-Epac1-camps(50A)* flies. Locomotor rhythms are highly sensitive to changes in the physiology or structure of PDF-expressing neurons (Nitabach et al., 2002, 2006; Helfrich-Förster, 1998; Park et al., 2000). Nevertheless, the behavior of flies expressing Epac1-camps in

these neurons was largely normal: they entrained to light:dark conditions (Figure S1B), and when released into constant darkness they exhibited persistent rhythmic activity (Table 1). Thus, Epac1-camps expression did not appear to disrupt the function of these neurons. We noted, however, that the period of the locomotor rhythm of these flies was significantly longer than those of controls (Table 1). We likewise evaluated the effect on circadian behavior of Epac1-camps expressed throughout the entire *Cry*-Gal4-positive network, but this experiment was confounded by the fact that the *Cry(39)-Gal4* element alone caused high levels of arrhythmicity under free-running conditions (Table 1). Nevertheless, under these conditions the expression of Epac1-camps resulted in no additional defects (Table 1). Importantly, these flies displayed a normal bimodal locomotor pattern under light:dark cycles (Figure S1G), which are the conditions under which cAMP imaging described here was performed.

Table 1. The Effect of Epac1-camps Expression on Free-Running Locomotor Rhythms

Genotype	n	% Rhythmic	τ (h) ± SEM
y w;;	31	77.4	23.3 ± 0.3
w^{1118};;	58	87.9	24.0 ± 0.1
w^{1118};uas-Epac1-camps(50A);	58	69.0	24.0 ± 0.1
Pdf(M)-Gal4;Sco/Cyo;	30	63.3	23.6 ± 0.2
Pdf(M)-Gal4;uas Epac1-camps(50A);	46	84.8	24.8 ± 0.4
uas- Epac1-camps(42A)$^{(w1118)}$;;	32	93.8	23.8 ± 0.1
y w;Cry(39)-Gal4;	27	18.5	25.3 ± 1.0
uas- Epac1-camps(42A)$^{(w1118)}$; Cry(39)-Gal4;	30	26.7	25.1 ± 0.9

The genotypes of wild-type flies, transgenic *uas-* and *Gal4*-lines, and combinations thereof are listed in the left column. For each genotype, we analyzed free-running behavior during days 3–9 of constant darkness and temperature after entrainment in 12:12 light:dark for 1 week. n is the number of flies for which sufficient data was collected to determine if each fly was rhythmic by chi-square periodogram analysis. For each genotype, the free-running period (τ) ± SEM resulting from chi-square periodogram analysis was calculated. By nonparametric ANOVA (Kruskal-Wallis Test), the period differences between *y w*, *w^{1118}*, *w^{1118};uas-Epac1-camps(50A)*, *Pdf(M)-Gal4;Sco/Cyo*; and *Pdf(M)-Gal4;uas- Epac1-camps(50A)* were highly significant ($p<0.0001$). Pairwise comparisons of *Pdf(M)-Gal4;uas- Epac1-camps(50A)* to parental stocks and wild-type controls indicated that this genotype displayed significantly longer periods than all other lines: $p < 0.05$ versus *w^{1118}*, $p < 0.001$ versus *y w*, $p < 0.001$ versus *Pdf(M)-Gal4;Sco/Cyo*, and $p < 0.01$ versus *w^{1118};uas-Epac1-camps(50A)*. All lines containing the *Cry(39)-Gal4* element were highly arrhythmic.

Epac1-camps in the l-vLNs Responds to Forskolin with a Loss of FRET

We next asked if this sensor displayed a cAMP-dependent reduction of FRET in the living fly brain. To evaluate the performance of the sensor, we first studied the cell bodies of the l-vLN pacemakers, due to their large size and superficial position. We recorded CFP donor and YFP FRET values for the l-vLNs of *Pdf(m)-Gal4/uas-Epac1-camps(42A)* female brains treated with 10 μM forskolin (FSK), an activator of most forms of adenylyl cyclase (de Souza et al., 1983). The l-vLNs responded to FSK with a 30%–50% loss of Epac1-camps FRET (Figures 1C and 1D; see Figure S2 for an explanation of the data analysis), consistent with an increase in cAMP concentration over a time course of 1 to 3 min. The time course of FSK-induced FRET loss was comparable in magnitude and latency to that seen for this sensor in stable cell lines in culture (Nikolaev et al., 2004) or in primary cells (Nikolaev et al., 2005). Importantly, this loss of FRET was not accompanied by a reduction of the intensity of YFP emission when excited directly with 475 nm light (data not shown), indicating that the reduction in FRET was not due to a loss of YFP fluorescence by photobleaching or nonspecific effects. Indeed, loss of YFP emission was accompanied by a parallel increase in CFP emission (Figure S2A). Vehicle addition was followed by an ~5% loss of FRET (Figure 1E,) as was the addition of dideoxyforskolin (ddFSK—Figure 1F), a biologically inactive form of FSK (de Rooij et al., 1998). These results indicate that transgenic Epac1-camps maintains its function as a cAMP sensor in living fly neurons.

The PDF-Expressing Large and Small vLNs Differ in Their Responsiveness to PDF

Using *pdf(M)-Gal4/uas-Epac1-camps(42A)* females, we next asked if the PDF-expressing l-vLNs and s-vLNs were responsive to PDF. The majority of l-vLNs displayed no clear response to 10^{-5} M PDF relative to vehicle controls (Figures 2A–2C). Two of 12 l-vLNs perhaps displayed a very small loss of Epac1-camps (Figure 2B). In contrast, the s-vLNs showed a pronounced loss of FRET in response to PDF compared to vehicle control (Figures 2D–2F). Indeed, PDF induced an ~30% loss of FRET in the s-vLNs (Figure 2F). Though every s-vLN tested responded to PDF with a loss of FRET, they did so with a wide range of latencies (see Discussion). We concluded that the s-vLNs responded to 10^{-5} M PDF with increases in cAMP but that the l-vLNs displayed little or no responsiveness. The PDF-induced loss of Epac1-camps FRET was also detectable in the dorsal projections of the s-vLNs (Figure S3), suggesting that the PDF-induced increases in cAMP spread throughout the neuron or are triggered at multiple subcellular locations.

The Response of the s-vLNs to PDF Is Dependent on PDF Concentration and Is Reversible

Having established that PDF responses could be measured using Epac1-camps, we created the stable *Pdf(m)-Gal4;uas-Epac1-camps(50A)* line to further characterize these responses. In this line, the cAMP response of the s-vLNs to PDF was dependent on peptide concentration. The magnitude of Epac1-camps FRET displayed concentration-dependent increases for PDF concentrations between 10^{-8} and 10^{-5} M (Figures 3A and 3B). Furthermore, the response of the s-vLNs to PDF was reversible. When treated with 10^{-6} M PDF, the s-vLNs displayed a prolonged loss of Epac1-camps FRET (Figure 3C). When a subset of these PDF-treated brains was rinsed with three 2000 μl volume exchanges of saline, they displayed a recovery to FRET levels that were indistinguishable from those of controls that had not been treated with PDF (Figure 3D). Following stimulus washout, Epac1-camps signal relaxation in the intact *Drosophila* brain proceeded over 5–6 min which, as expected from the kinetic

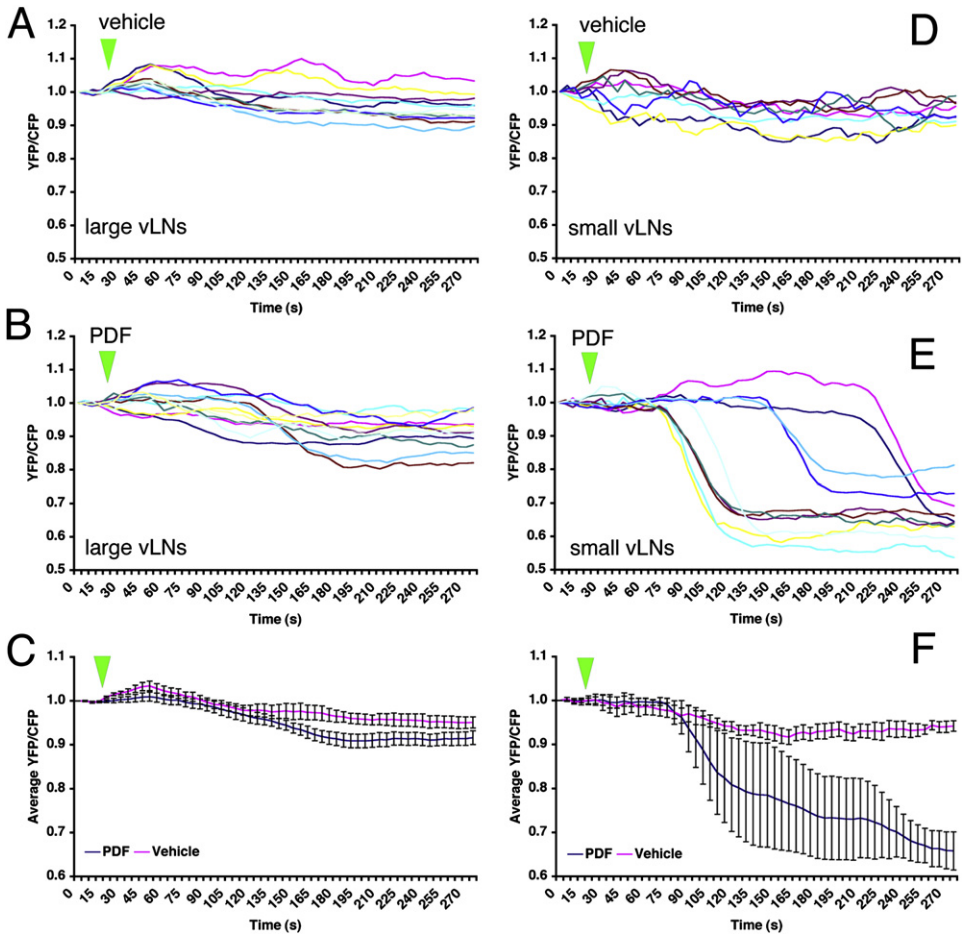

Figure 2. The s-vLNs of *pdf(M)-Gal4/uas-Epac1-camps(42A)* Flies Display a Pronounced Loss of FRET in Response to 10^{-5} M PDF

(A–F) FRET plots for the cell bodies of l-vLNs and s-vLNs in vehicle- and PDF-treated brains. (A) FRET plots for eleven l-vLNs from four brains treated with vehicle. Green triangles indicate the start of bath application. (B) FRET plots for 12 l-vLNs from four brains treated with 10^{-5} M PDF. (C) Average FRET plots for l-vLNs of brains treated with vehicle and PDF. (D) FRET plots for eight s-vLNs from four brains treated with vehicle. (E) FRET plots for ten s-vLNs from five brains treated with 10^{-5} M PDF. (F) Average FRET plots for s-vLNs of brains treated with vehicle and PDF. A two-way, repeated-measures ANOVA was performed on these data with fixed factors cell type (l-vLNs versus s-vLNs) and peptide (PDF versus vehicle) using all time measurements as within-subjects factors. There was a significant within-subject effect of time ($p < 0.001$), a significant between-subjects effect of the cell type ($p < 0.001$), and PDF was significantly different than vehicle ($p < 0.001$).

limitations in washout from intact brains, is slower than that observed in cultured cells (Nikolaev et al., 2004). Brains that were "mock-washed" with 10^{-6} M PDF maintained low FRET levels for the duration of the experiment (Figure 3D).

A Peptide Screen Reveals Receptivity to DH31 in the l-vLNs and s-vLNs

As an initial screen for modulators of cAMP in the PDF-positive vLNs, we observed the time course of Epac1-camps FRET in the l-vLNs and s-vLNs of *Pdf(m)-Gal4;uas-Epac1-camps(50A)* brains following bath application of a suite of neuropeptides delivered at 10^{-6} M. As expected, the s-vLNs displayed an approximately 30% loss of FRET in response to 10^{-6} M PDF (Figures 3E and S4E), while the l-vLNs showed no pronounced response to PDF (Figures 3F and S4B). In contrast, both the l-vLNs and s-vLNs displayed large FRET decreases in response to the calcitonin-related peptide diuretic hormone 31 (DH31) (Figures 3E and 3F and S4C and S4F). The profile of DH31-induced FRET loss in the l-vLN was larger, more precipitous, and more prolonged compared to that in s-vLNs (compare Figures S4C and S4F). As for PDF in the s-vLNs, the response to DH31 displayed a wide range of latencies in the l-vLNs and s-vLNs. Relatively small or no FRET changes where observed for the remainder of the neuropeptides tested (Figures 3E and 3F), with the l-vLNs displaying a brief, small, and transient loss of FRET in response to diuretic hormone 44 (Figure 3F).

The Response to PDF in the s-vLNs Requires PDFr

The Epac1-camps reporter indicated that the vLNs responded with cAMP increases to both PDF (s-vLNs only) and to DH31 (both l-vLNs and s-vLNs). These results suggested the actions of specific PDF and DH31 receptor populations. cAMP-based

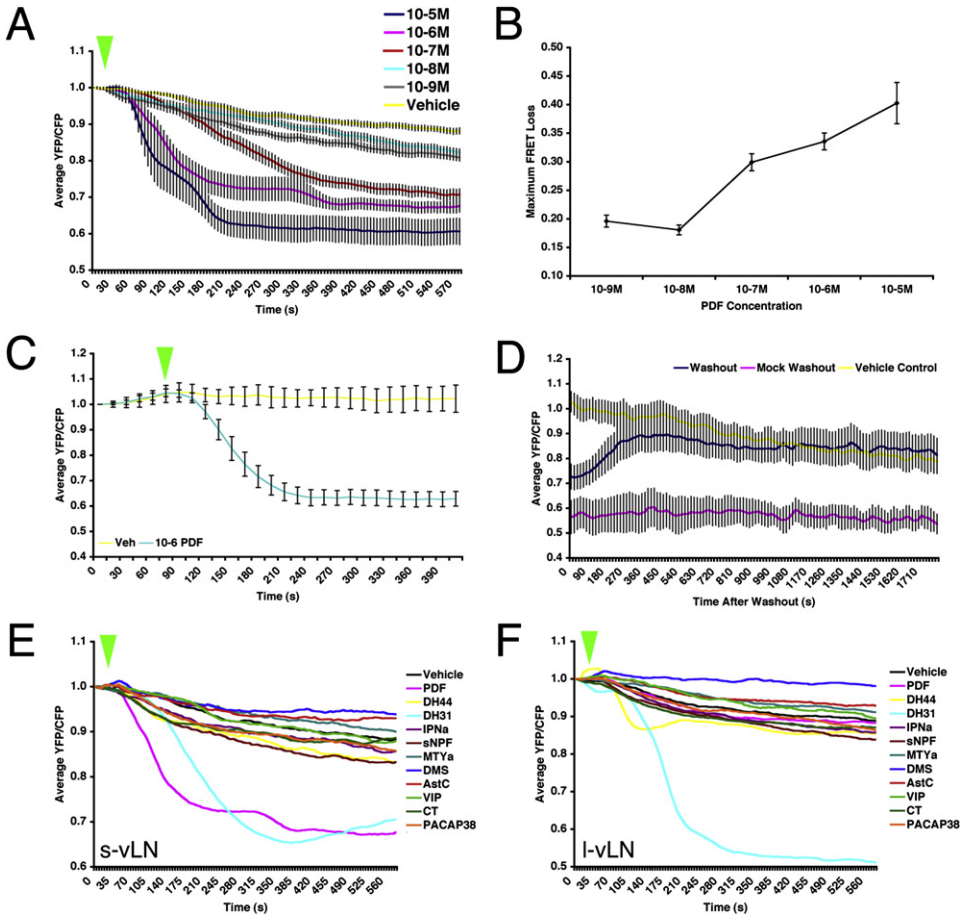

Figure 3. PDF-Induced Loss of Epac1-camps FRET Is Dependent on the PDF Concentration and Is Reversible; the Neuropeptide DH31 Triggers Similar Effects

(A) Average plots of FRET following bath application of various concentrations of PDF in the s-vLNs of *Pdf(m)-Gal4;uas-Epac1-camps(50A)* brains. Green triangles represent the start of peptide exposure. The effects of different PDF concentrations were compared by repeated-measures ANOVA using PDF concentration as the fixed factor. This test indicated a significant effect of the PDF concentration on FRET Loss over time ($p > 0.001$).

(B) A comparison of average maximum Epac1-camps FRET loss in response of increasing concentrations of PDF from the same experiment shown in (A). Maximum FRET loss was determined for each neuron as shown in Figure S2. A single-factor ANOVA revealed that PDF concentration had a significant effect on the level of maximum FRET loss ($p < 0.001$).

(C) Average FRET plots for s-vLNs from *Pdf(m)-Gal4;uas-Epac1-camps(50A)* brains treated with 10^{-6} M PDF or vehicle. The plots are based on 14 neurons from 14 brains for PDF treatment and five neurons from five brains for vehicle. Images were captured every 15 s.

(D) Time-course of FRET for the cells shown in (C) following washout of PDF, or mock-washout in which the original 10^{-6} M PDF was removed then immediately reintroduced. Vehicle-treated cells from (C) were also imaged following a rinse identical to that for the washout. The plots are based on nine neurons from nine brains for washout, five neurons from five brains for mock-washout, and five neurons from five brains for vehicle. Time points were taken every 15 s. A repeated-measures ANOVA revealed a significant effect of washout ($p = 0.002$) and that PDF washout cells were statistically homogenous with control cells by Tukey HSD.

(E) Average plots of FRET in s-vLNs of *Pdf(m)-Gal4;uas-Epac1-camps(50A)* brains following exposure to one of a suite of fly and vertebrate peptides at 10^{-6} M. Error bars have been omitted to display all plots with clarity. Application of both PDF (magenta) and DH31 (light blue) resulted in pronounced loss of FRET in the s-vLNs. A one-way repeated-measures ANOVA was performed. Though there was a significant effect of peptide treatment ($p < 0.001$), only the PDF and DH31 treatments were statistically distinct from controls by Tukey HSD.

(F) Average plots of FRET in l-vLNs of *Pdf(m)-Gal4;uas-Epac1-camps(50A)* brains following exposure to one of a suite of fly and vertebrate peptides at 10^{-6} M. Error bars have been omitted to display all plots with clarity. A one-way repeated-measures ANOVA was performed. Though there was a significant effect of peptide treatment ($p < 0.001$), only the DH31 and dromyosuppressin (DMS) treatments were statistically distinct from controls by Tukey HSD. The data summarized in (E) and (F) are based on observations on five to 14 neurons of each class from three to five brains for each peptide. Individual plots for vehicle-, PDF-, and DH31-treated l-vLNs and s-vLNs are shown in Figure S4.

signaling assays following functional expression of the GPCRs in vitro showed that PDFr responds strongly to PDF and moderately to DH31 (Mertens et al., 2005), while DH31r responds strongly to DH31 and not at all to PDF (Johnson et al., 2005). We therefore wished to determine in vivo the extent to which PDFr was required for responses to the PDF and DH31 neuropeptides. To this end, we conducted Epac1-camps FRET imaging plots in the l-vLNs and s-vLNs of han^{5304} flies bearing a large C-terminal deletion of PDFr, a mutation that produces a behavioral phenocopy to the pdf^{01} peptide mutant (Hyun et al.,

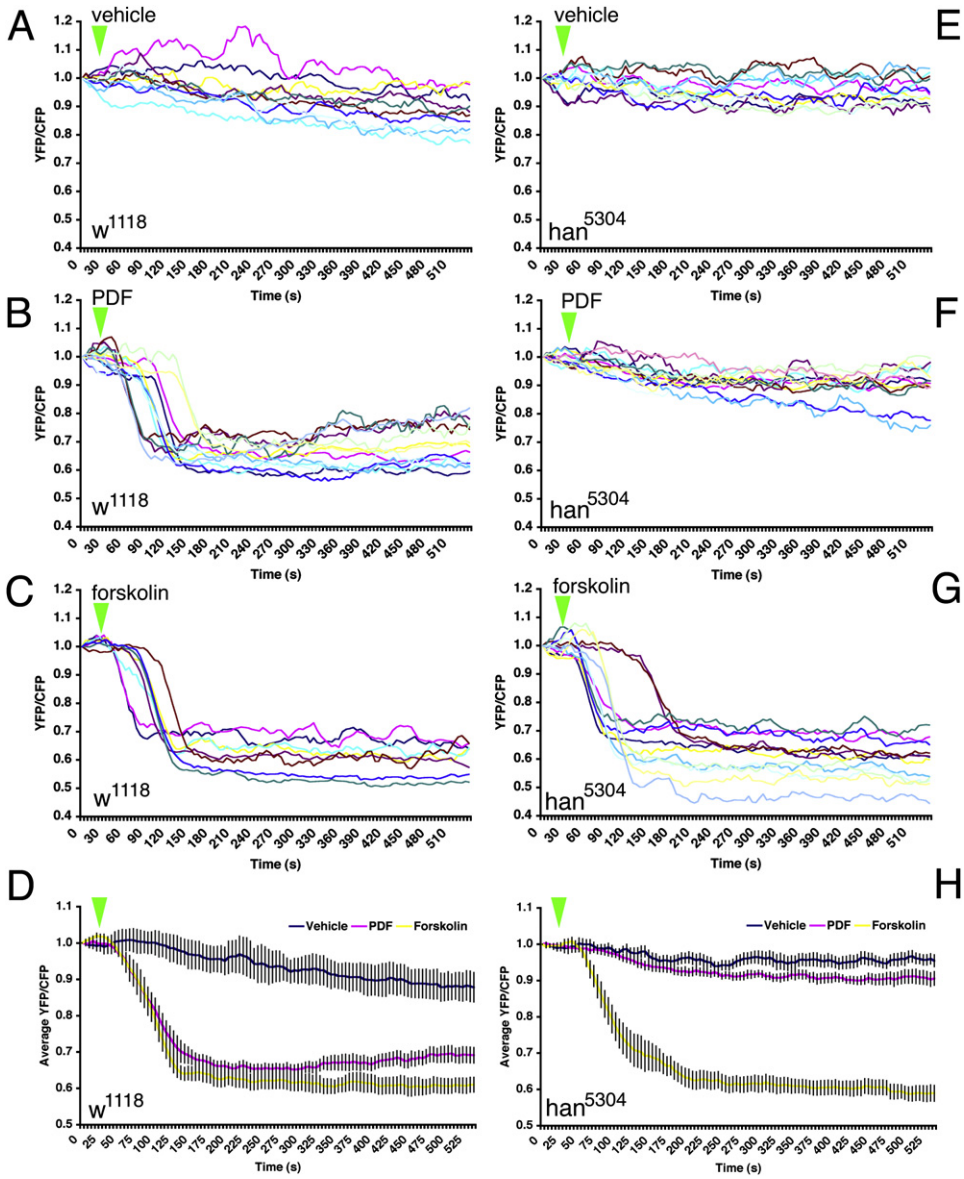

Figure 4. The Response to PDF in the s-vLNs Requires PDFr

(A) FRET plots for ten *w*^{1118}*; pdf(bmrj)-Gal4/uas-Epac1-camps(50A)* (wild-type) s-vLNs from five brains treated with vehicle. Green triangles indicate the start of bath application.

(B) FRET plots for 13 wild-type s-vLNs from six brains treated with 10^{-5} M PDF.

(C) FRET plots for eight wild-type s-vLNs from five brains treated with 10 μM FSK.

(D) Average FRET plots for vehicle, PDF, and FSK application in wild-type brains. Both PDF and FSK induced pronounced FRET loss.

(E) FRET plots for 11 *han*^{5304}*; pdf-Gal4/uas-Epac1-camps(50A)* (*pdfr* mutant) s-vLNs from five brains treated with vehicle.

(F) FRET plots for 14 *pdfr* mutant s-vLNs from six brains treated with 10^{-5} M PDF.

(G) FRET plots for 13 *pdfr* mutant s-vLNs from five brains treated with 10 μM FSK.

(H) Average FRET plots for vehicle, PDF, and FSK application in *pdfr* mutants. A two-way repeated-measures ANOVA using genotype and drug/peptide treatment as fixed factors revealed a significant effect of genotype and drug, as well as a significant interaction (i.e., the genotypes are both affected by the drugs, but in different ways). The means across all values of time of the three drug treatments are statistically distinct (i.e., control is different from FSK which is different from PDF).

2005). First, we considered the responses to PDF in the s-vLNs. As expected, the s-vLNs of control flies (*w*^{1118}*/y;BMRJ-Gal4/uas-Epac1-camps50A*) showed a clear, ~30% maximum loss of Epac1-camps FRET in response to 10^{-5} M PDF (Figures 4B and 4D). In *han*^{5304}mutant flies (*han*^{5304}*/y;BMRJ-Gal4/uas-Epac1-camps(50A)*), there was no comparable Epac1-camps FRET loss in response to 10^{-5} M PDF (Figures 4F and 4H). The s-vLNs in both mutant and control lines showed a clear and

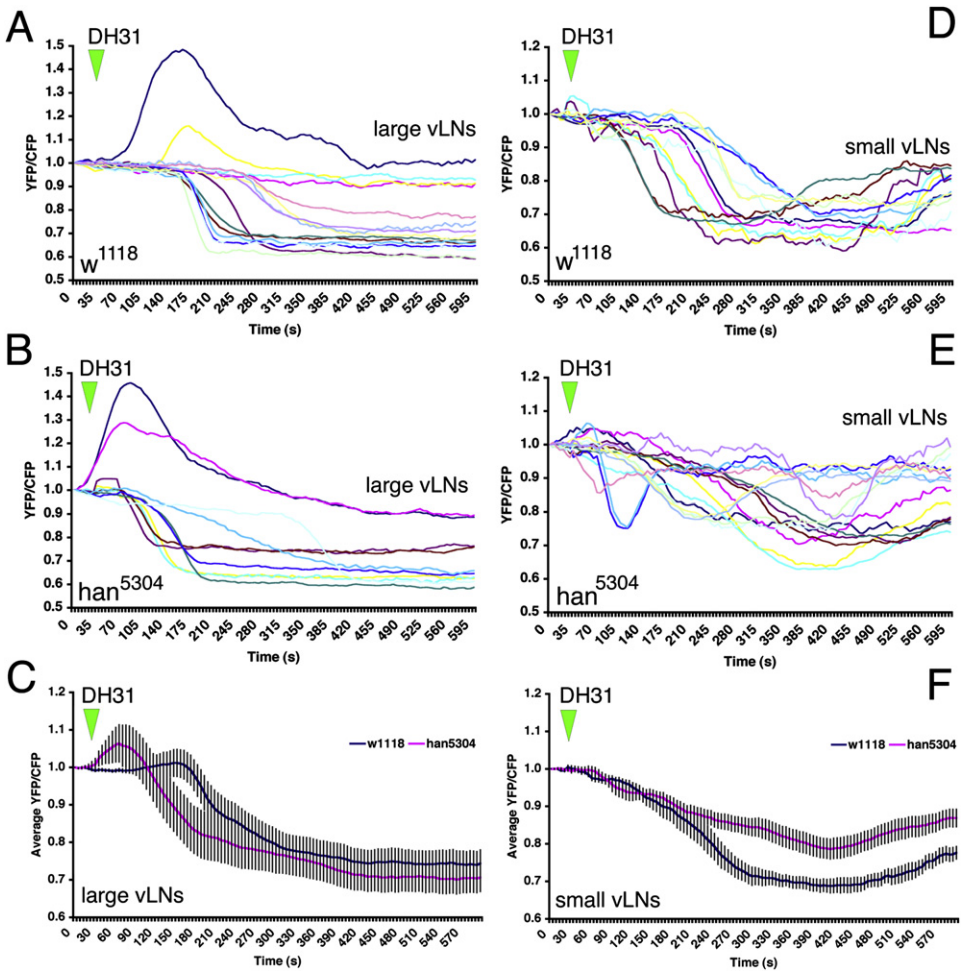

Figure 5. Responsiveness to DH31 in the l-vLNs and s-vLNs Does Not Require PDFr, but Is Reduced in the s-vLNs of the pdfr Mutant *han*^{5304}

(A) Epac1-camps FRET plots for 15 control [*w1118/y; pdf-Gal4/uas-Epac1-camps(50A)*] l-vLNs from six brains treated with 10^{-6} M DH31. Green triangles indicate the start of bath application.

(B) Epac1-camps FRET plots for ten *han*^{5304}*/y; pdf-Gal4/uas-Epac1-camps(50A)* (*pdfr* mutant) l-vLNs from six brains treated with 10^{-6} M DH31.

(C) Average plots of the DH31 response of the l-vLNs of wild-type and *pdfr* mutant brains.

(D) Epac1-camps FRET plots for 11 control s-vLNs from five brains treated with 10^{-6} M DH31.

(E) Epac1-camps FRET plots for 15 *pdfr* mutant s-vLNs from seven brains treated with 10^{-6} M DH31.

(F) Average Epac1-camps FRET plots response of the s-vLNs of wild-type and *pdfr* mutant brains. Despite the clear trend toward reduced FRET loss in the s-vLNs of *pdfr* mutants, a repeated-measures two-way ANOVA with main effects factors genotype and neuronal type found no significant effect of genotype ($p = 0.571$). There was a marginally significant interaction ($p = 0.056$) indicating that the trend in FRET response behavior differs between l-vLNs and s-vLNs is reversed for the two genotypes considered (*w*^{1118} and *han*^{5304}).

comparable loss of FRET in response to forskolin (Figures 4C, 4D, 4G, and 4H), suggesting that the lack of PDF response in the *han*^{5304} background was not due to deficiencies in cAMP signaling but rather to the loss of PDFr.

Next, we analyzed responses to DH31. In control flies, 13 of 15 l-vLNs displayed a loss of Epac1-camps FRET in response to DH31; the remaining two cells displayed a transient increase in FRET (Figure 5A). The responses to DH31 in the l-vLNs of *han*^{5304} mutant flies were very similar to those observed in the control line; the majority of l-vLNs displayed a loss of FRET, while two others displayed transient increases (Figure 5B). Thus, the DH31 response in the l-vLNs did not require PDFr. In contrast, the response to DH31 by the s-vLNs was correlated with *pdfr* genotype (Figures 5D and 5E), though the effects were modest. As expected, s-vLNs in control *w*^{1118} flies showed a clear loss of FRET in response to DH31 but with onset and recovery profiles that often differed from those of the l-vLNs (compare Figures 5A and 5D). The s-vLNs of *han*^{5304}mutant flies responded differently to DH31 than did those cells in wild-type controls (Figures 5E and 5F). For example, the average FRET loss in response to DH31 was 30% in the wild-type *w*^{1118} background but only 20% in *han*^{5304} mutants (Figure 5F). Furthermore, *han*^{5304} mutant s-vLNs displayed a range of Epac1-camps FRET profiles after DH31 addition: some showed a brief, shallow loss of FRET that varied in duration and onset, whereas others displayed little or no response to DH31 (Figure 5E). Thus, in the absence of

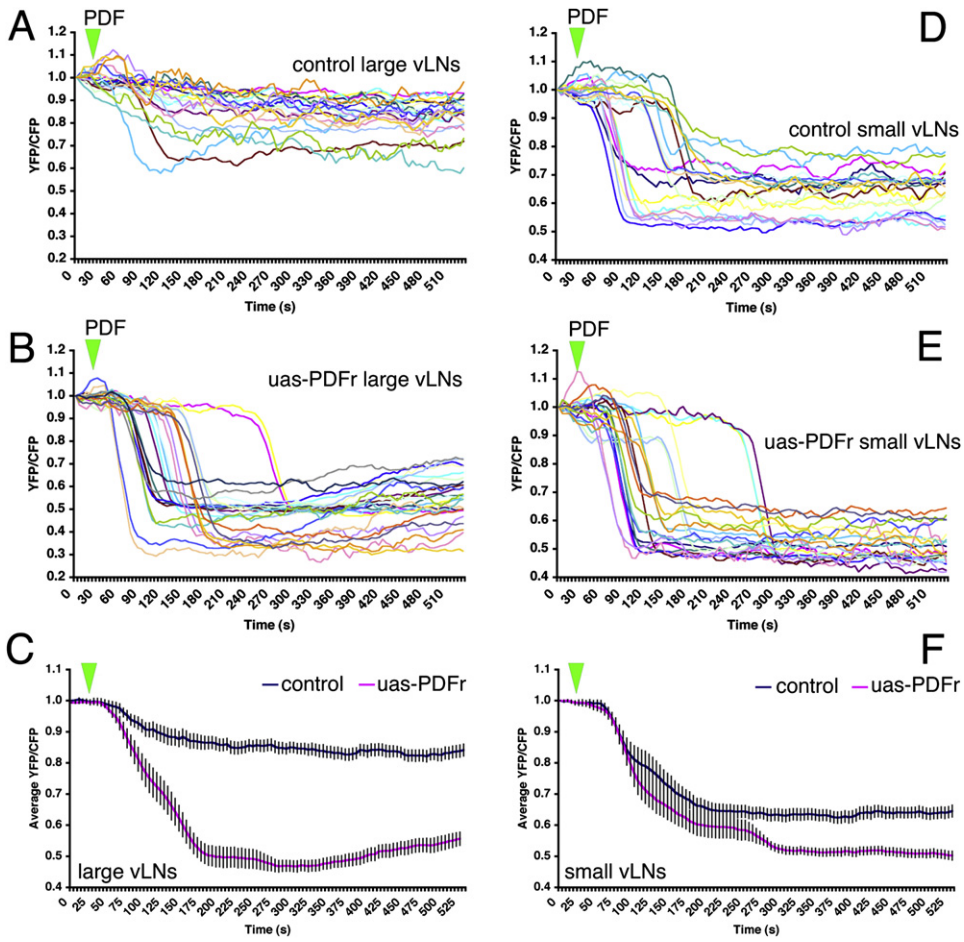

Figure 6. uas-Driven PDFr Expression Confers Pronounced PDF Responsiveness upon the l-vLNs and Increases the PDF Response of the s-vLNs

(A) FRET plots of 21 *Pdf(m)-Gal4;uas-Epac1-camps(50A)/Cyo* (control) l-vLNs from 10 brains treated with 10^{-5} M PDF. Green triangles indicate the time of bath application.

(B) FRET plots of 25 *Pdf(M)-Gal4/uas-Epac1-camps(50A)/uas-PDFr(16L)* (PDFr overexpressing) l-vLNs from 11 brains treated with 10^{-5} M PDF.

(C) Average FRET plots from wild-type and PDFr-overexpressing (uas-*PDFr*) l-vLNs.

(D) FRET plots of 20 wild-type s-vLNs from 10 brains treated with 10^{-5} M PDF.

(E) FRET plots of 23 PDFr overexpressing s-vLNs from 12 brains treated with 10^{-5} M PDF.

(F) Average FRET plots from control and PDFr-overexpressing s-vLNs. A two-way repeated-measures ANOVA with factors cell-type and PDFr expression revealed a significant effect of all between-subjects factors (PDFr and cell type) and a significant interaction indicating that the two cell types responded differently to PDFr overexpression.

PDFr, the DH31 responses in the s-vLNs were changed, consistent with a hypothesis that both PDFr and a separate DH31r (Johnson et al., 2005) underlie the observed DH31 response in wild-type s-vLNs.

Gal4-Driven Expression of PDFr in the l-vLNs and s-vLNs Confers Responsiveness to PDF in l-vLNs and Increases It in the s-vLNs

The s-vLNs in wild-type flies showed large cAMP increases in response to PDF while the l-vLNs did so rarely and with low magnitude (Figures 2 and S4B). This is consistent with the hypothesis that PDFr is expressed in s-vLNs but not the l-vLNs. We tested the sufficiency of PDFr to confer responsiveness to PDF through *pdfr* misexpression in the l-vLNs and s-vLNs in an otherwise wild-type *PDFr* background (using GAL4 misexpression in *Pdf(m)-Gal4/y;uas-PDFr(16L)/uas-Epac1-camps(50A)* flies. By design, we intended both the l-vLNs and s-vLNs to express high levels of PDFr in addition to any native PDFr. Thus, we asked whether this manipulation conferred some (or more) responsiveness to PDF in the vLNs.

The response of control (*Pdf(m)-Gal4/y;uas-Epac1-camps(50A)/Cyo*) l-vLNs to 10^{-5} M PDF is shown in Figure 6A. Two l-vLNs displayed a clear loss of FRET, but the majority (n = 47) did not (Figure 6A). In contrast, every l-vLN in the misexpressing PDFr genotype displayed a large FRET change in response to PDF (Figure 6B). The addition of PDFr conferred a pronounced PDF receptivity onto the l-vLNs (Figure 6C). As expected, every s-vLN in control flies displayed a loss of FRET following PDF application

(Figure 6D). The addition of uas-pdfr increased the PDF-induced FRET loss in the s-vLNs from 35% to 40% (Figures 6D and 6E). The shapes and latencies of PDF-induced FRET loss in s-vLNs were not correlated with genotype (Figures 6D and 6E). These observations are consistent with the hypothesis that the PDF response in wild-type s-vLNs is direct and limited by the amount of PDFr expressed.

There Is Widespread PDF Receptivity throughout the Circadian Clock Neuron Network of *Drosophila*

Two independent anti-PDFr sera have been described that differ in the extent to which they react with the various classes of clock neuron (Hyun et al., 2005; Mertens et al., 2005). Hyun and colleagues (2005), using antisera raised against an N-terminal sequence of PDFr, reported immunoreactivity in the l-vLNs, $DN1_p$s, and in a single dLN. In contrast, Mertens and colleagues (2005), using sera raised against a C-terminal sequence, described PDFr expression in the $DN1_a$s, but not in the dLNs, l-vLNs, or the $DN1_p$s. These reports employed different microscopy methods to visualize PDFr immunoreactivity. We therefore wondered if the differing level of resolution employed by these two studies (Hyun et al. [2005] and Mertens et al. [2005]) could explain these apparent differences in PDFr expression. To this end, we performed ant-PDFr immunocytochemistry using both anti-N and anti-C-terminal PDFr sera with high-resolution laser confocal microscopy. Our results indicated a general lack of PDFr immunoreactivity among clock neurons and a lack of consensus between the two sera (Figure S5). As previously reported by Hyun and colleagues (2005), the N-terminal sera revealed the l-vLNs (Figures S5J–S5L). Nevertheless, we found no evidence for PDFr immunoreactivity among the $DN1_p$s and dLNs but did detect PDFr immunoreactivity in cells quite close to these clock neurons (Figures S5C, S5F, S5Y, and S5BB). Furthermore, we found no evidence of a diminution of l-vLN PDFr signals in the han^{5304} deletion mutant (Figure S5CC; Hyun et al., 2005). Under these same imaging conditions, we found that the $DN1_a$s were immunoreactive to anti-C-terminal sera and like the anti-N-terminal sera, revealed soma close to the dLNs and $DN1_p$s (Figures S5B and S5Y; Mertens et al., 2005). We have detected no neurons whose immunoreactivity (to either serum) is reduced or abrogated in the han^{5304} mutant (data not shown). We concluded that existing anti-PDFr sera offer no genetically-verifiable data concerning PDFr expression within the CNS.

We therefore used Epac1-camps to begin mapping PDF receptivity throughout the clock neuron network. The *Cry(39)-Gal4* element directed Epac1-camps expression throughout all clock neuron classes, except the lateral posterior neurons (Figure 1B). The fifth s-vLN was specifically visualized with *Cry(39)-Gal4* in conjunction with *uas-Epac1-camps(42A)* and *Pdf-Gal80*, with the latter element reducing Epac1-camps intensity in the PDF-positive vLNs (data not shown).

All non-PDF-expressing clock neuron classes tested here displayed pronounced and statistically significant FRET loss in response to 10^{-6} M PDF relative to vehicle controls (Figure 7; detailed data for each clock neuron class can be found in Figures S6 and S7). All fifth s-vLNs responded to 10^{-6} M PDF with a clear loss of FRET (Figure S6A). Responses by fifth s-vLNs showed a range of latencies. The majority (20/24) of dLNs responded to PDF with a significant loss of FRET (Figure S6C).

Eleven of twelve $DN1_a$s responded to PDF with a loss of FRET (Figure S7A), as did the vast majority of $DN1_p$s (Figure S7C). Unlike all other clock neurons tested in this study, vehicle-treated $DN1_p$s displayed remarkably unstable FRET levels (Figure S7D), suggesting dynamic endogenous cAMP signaling. The DN2s displayed comparatively small but significant losses of FRET (Figure S7E). Ten of 11 l-DN3s responded to PDF with a loss of FRET (Figure S7G). There was a significant difference between PDF and vehicle treatment in these cells despite the relatively large amount of FRET loss observed in vehicle controls (Figures 7F, S7G, and S7H) in these cells.

We could not test the responses of non-vLN pacemakers in the han^{5304} mutant flies because they displayed extremely low Epac1-camps expression levels in the han^{5304} background (data not shown). Nevertheless, our results establish that receptivity to PDF is widespread throughout most elements of the circadian clock network.

Our data suggest that the l-vLNs are unique among the clock neurons tested here, in that the vast majority failed to respond to PDF. Indeed, only three of 23 wild-type l-vLNs responded to bath applied 10^{-5} M PDF with a clear, though small, loss of FRET (Figures 2B and 6B), and no l-vLNs showed clear responses to 10^{-6} M PDF (Figure S4B). It is possible that the few l-vLNs that displayed small cAMP increases in response to PDF represented a low incidence of PDFr expression in the l-vLNs. But it is also possible, due to the relatively poor axial resolution of standard reflective epifluorescent microscopy, that the measured Epac1-camps FRET loss in these few cells may have been due to light "contamination" from nearby s-vLNs because, in many brains, the l-vLNs and s-vLNs were closely situated. To test for this possibility, we replicated the responses of l-vLNs and s-vLNs to 10^{-5} M PDF in *Pdf(m)-Gal4;uas-Epac1-camps* brains using the confocal microscope, the superior axial resolution of which allowed us to exclude CFP and YFP emission above and below the focal plane. Confocal pinhole apertures were set to attain optical section thicknesses of less than 1 μm. As expected, all s-vLNs responded to 10^{-5} M PDF with a pronounced loss of Epac1-camps FRET (Figures 8B and 8C). The majority (18 of 20) of l-vLNs showed no response to 10^{-5} M PDF, but two cells displayed clear but small Epac1-camps FRET loss. We conclude that the low-frequency responses to PDF among the l-vLNs that we observed under the epifluorescent microscope are not explained by light contamination from the s-vLNs.

We were also concerned with the verity of the PDF-induced FRET loss observed in the DN2s. We worried that these FRET changes might have been derived from nearby projections of other Epac1-camps-expressing clock neurons. For example, the DN2 abut the terminals of the dorsal projections of the ispilateral s-vLNs. These projections display a pronounced loss of Epac1-camps FRET following PDF addition (Figure S3). To ensure that the PDF-induced FRET losses emanated from the DN2 soma and not from nearby clock neuron projections residing above or below the DN2 focal plane, we repeated the PDF plots for DN2s in *uas-Epac1-camps(42A);Cry(39)-Gal4* brains using the confocal. Under these imaging conditions, every DN2 showed a clear loss of Epac1-camps FRET in response to

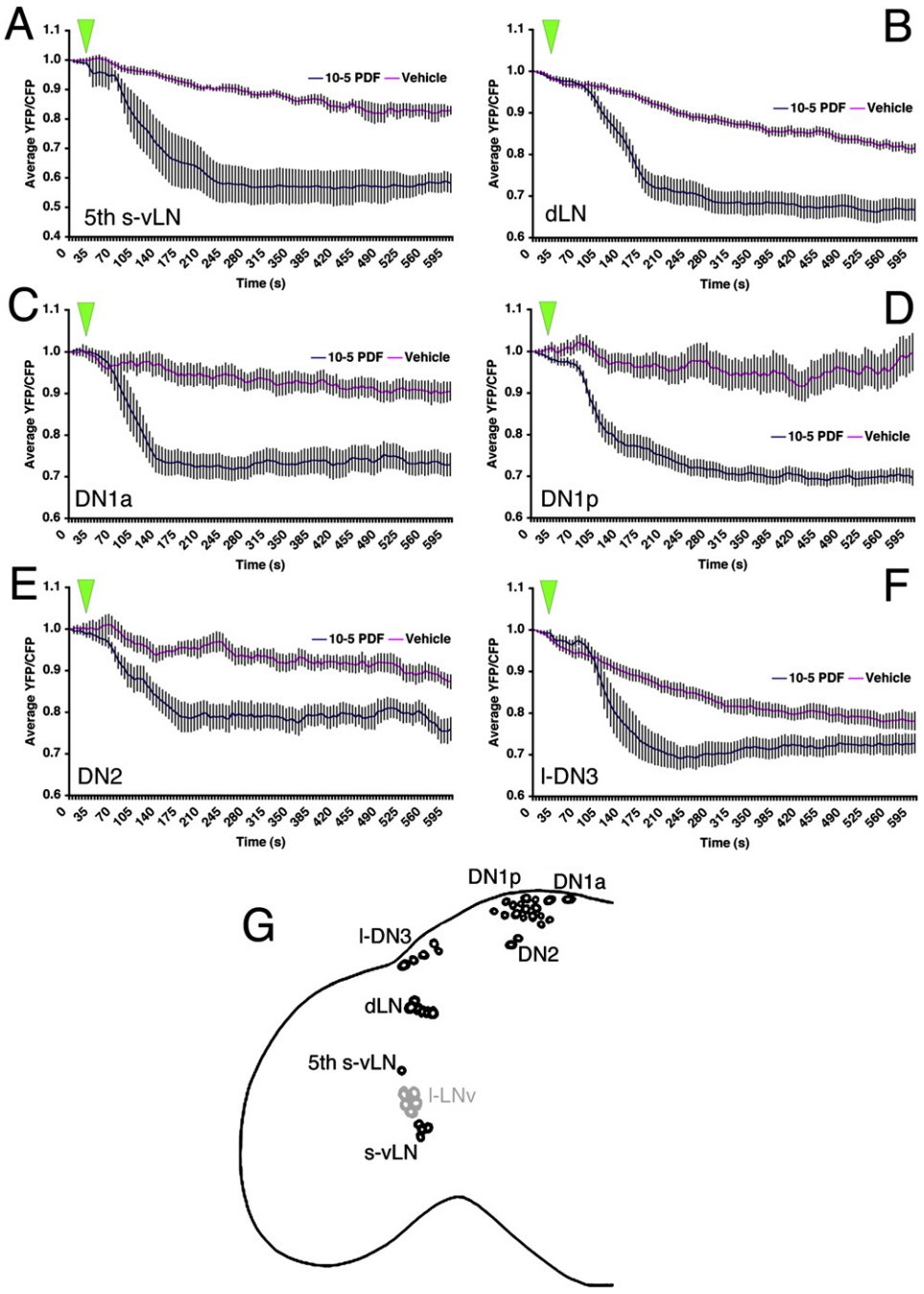

Figure 7. All Classes of PDF-Negative *Cry(39)-Gal4*-Positive Clock Neurons Display Increased cAMP in Response to 10^{-5} M PDF

The response of the 5th s-vLN was tested in *uas-Epac1-camps(42A);Cry(39)-Gal4/Pdf-Gal80* males. All other clock neurons were tested in *uas-Epac1-camps(42A);Cry(39)-Gal4* males.

(A) Average plots of Epac1-camps FRET in the fifth s-vLNs following bath application of 10^{-5} M PDF or vehicle. Green triangles represent start of bath application.

(B) Average plots of Epac1-camps FRET in dLNs following bath application of 10^{-5} M PDF or vehicle.

(C) Average plots of Epac1-camps FRET in the DN1a following bath application of 10^{-5} M PDF or vehicle.

(D) Average plots of Epac1-camps FRET in the DN1p following bath application of 10^{-5} M PDF or vehicle.

(E) Average plots of Epac1-camps FRET in the DN2 following bath application of 10^{-5} M PDF or vehicle.

(F) Average plots of Epac1-camps FRET in the l-DN3 following bath application of 10^{-5} M PDF or vehicle. Individual cell responses for the different circadian cell groups are shown in the following figures: fifth s-vLN (Figures S6A and S6B), dLN (Figures S6C and S6D), DN1a (Figures S7A and S7B), DN1p (Figures S7C and S7D), DN2 (Figures S7E and S7F); large-DN3 (Figures S7G and S7H).

(G) A schematic representation of PDF receptivity throughout eight classes of circadian clock neuron. Black cells indicate the neurons that displayed consistent FRET loss in response to PDF in this study. Gray cells indicate neurons that displayed little or no responses to PDF. The small DN3 cells were not tested. Data were

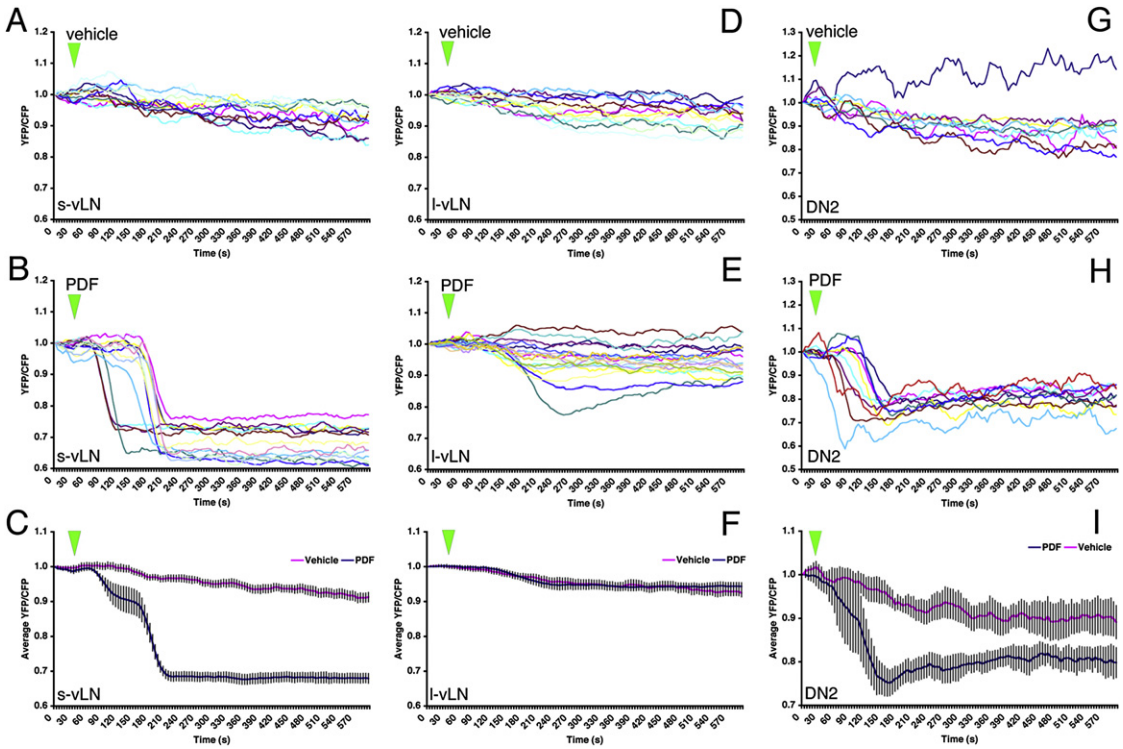

Figure 8. Confocal Imaging of Epac1-camps FRET following Bath Application of 10^{-5} M PDF in the s-vLNs, l-vLNs, and DN2s

(A) Epac1-camps FRET plots for eleven s-vLNs from seven *Pdf(m)-Gal4;uas-Epac1-camps(50A)* brains treated with vehicle.

(B) Epac1-camps FRET plots for 14 s-vLNs from seven *Pdf(m)-Gal4;uas-Epac1-camps(50A)* brains treated with 10^{-5} M PDF.

(C) Average Epac1-camps FRET plots response of the s-vLN to vehicle (magenta) and PDF (blue), imaged with the confocal.

(D) Epac1-camps FRET plots for 12 l-vLNs from seven *Pdf(m)-Gal4;uas-Epac1-camps(50A)* brains treated with vehicle.

(E) Epac1-camps FRET plots for 20 l-vLNs from ten *Pdf(m)-Gal4;uas-Epac1-camps(50A)* brains treated with 10^{-5} M PDF.

(F) Average Epac1-camps FRET plots response of the l-vLN to vehicle and PDF, imaged with the confocal. Data for the s- and l-vLNs were analyzed by repeated-measures ANOVA with two fixed factors: cell-type and PDF treatment. This test revealed a significant effect of 10^{-5} M PDF as well as a significant effect of neuronal type. In addition, there was a significant ($p = 0.01$) interaction between neuronal type and peptide treatment indicating that the different neuronal types respond differently to 10^{-5} M PDF.

(G) Epac1-camps FRET plots for nine DN2s from seven *uas-Epac1-camps(42A);Cry(39)-Gal4* brains treated with vehicle.

(H) Epac1-camps FRET plots for ten DN2s from six *uas-Epac1-camps(42A);Cry(39)-Gal4* brains treated with 10^{-5} M PDF.

(I) Average Epac1-camps FRET plots response of the DN2s to vehicle and PDF, imaged with the confocal. A one-way repeated-measures ANOVA revealed that the effect of PDF on the DN2s was highly significant ($p = 0.001$).

bath-application of 10^{-5} M PDF (Figure 8H). We therefore concluded that this FRET loss indeed reflected a response of the DN2s and not nearby neuronal projections.

DISCUSSION

Epac1-camps Sensor Maintains Its Function in the Living Fly Brain

The recently-developed Epac-based cAMP sensors have made it possible to monitor cAMP levels with unprecedented temporal resolution and sensitivity (Nikolaev et al., 2004; DiPilato et al., 2004; Ponsioen et al., 2004). These sensors have been used to observe cAMP dynamics in cell culture (Landa et al., 2005; Willoughby and Cooper, 2006; Ponsioen et al., 2007), in cardiomyocytes from mice transgenic for a similar sensor (Nikolaev et al., 2006), and in the explanted neonatal retina (Dunn et al., 2006). Here, we have shown that Epac1-camps (Nikolaev et al., 2004) is a functional cAMP sensor within identified neurons of the adult brain of transgenic *Drosophila*. In response to certain *Drosophila* bioactive peptides like PDF, the s-vLNs displayed dramatic and long-lasting deceases in the FRET signal that were consistent with a rise in intracellular cAMP. The sensor displays high selectivity in vitro, with a much higher affinity for cAMP than for cGMP (Nikolaev et al., 2004). In addition, PDFr activation triggers a rise in $[cAMP]_{intra}$ (Hyun et al., 2005). Thus, while we cannot exclude the possibility that changes in cGMP

analyzed by two-way repeated-measures ANOVA with factors cell-type and PDF treatment. There was a significant effect of both main effects factors (PDF versus vehicle; pacemaker cell type, $p < 0.001$ in both cases) on Epac1-camps FRET of all cell classes. A significant interaction ($p = 0.031$) suggests that the pacemaker cells respond differently to PDF application.

or other intracellular messengers may contribute to some of the measurements, it is very likely the signal is due to changes in intracellular cAMP content.

The s-vLNs but Not the l-vLNs Respond to PDF

Every wild-type s-vLN tested in this study (n = 56) displayed cAMP increases in response to PDF at concentrations $\geq 10^{-6}$ M. We note that the scale of the PDF-induced cAMP increases in the s-vLNs rivaled those of forskolin, suggesting that PDFr may normally exert large-scale effects on cAMP levels in these cells. The magnitude of PDF-induced loss of Epac1-camps FRET was dependent on the concentration of the peptide and the expression level of PDFr, indicating that our methods here are sensitive enough to measure not only the presence but the extent of PDFr signaling in within identified neurons. The PDF response was absent in the s-vLNs of *han*^{5304} mutants, indicating that it required PDFr. Furthermore, driving additional PDFr expression in the s-vLNs increased the magnitude of the cAMP responses but not their latencies. This is consistent with the hypothesis that s-vLNs normally express PDFr. In contrast, the majority of wild-type l-vLNs tested in this study (43 of 46 neurons) showed no clear cAMP increases in response to 10^{-6}–10^{-5} M PDF, suggesting a lack of PDF receptivity in this class of clock neuron. One explanation for the low frequency of PDF receptivity among the l-vLNs is a low incidence of PDFr or another receptor with some sensitivity to PDF. Alternatively, these infrequent and relatively small PDF responses may represent indirect effects of PDF through synaptic intermediaries. Nevertheless, it is clear that the l-vLNs are unique among the clock neuron classes tested, with the vast majority displaying no response to PDF.

The degree to which PDFr signaling displays desensitization is of interest to understand its role in the synchronization of circadian neural circuits. Following functional expression in cell lines, several *Drosophila* GPCRs (including family B type GPCRs) undergo internalization within 1 to 5 min (Johnson et al., 2003, 2004). It was notable therefore that, while the change in the FRET signal in response to PDF was quickly reversed with washout, the change was sustained for as long as free peptide remained in the bath (for a period >28 min). Therefore, real-time measurements of PDF signaling in s-vLNs within the intact brain reveal little if any FRET recovery with long-term exposure to agonist.

Our data are consistent with presence of functional PDF autoreceptors expressed by the PDF-expressing s-vLNs. While the concept of autoreceptors is well established for conventional transmitters, there is also evidence to suggest that peptide autoreceptors help shape the normal pattern and amount of neuropeptide release. Somatostatin inhibits its own secretion in hypothalamic periventricular neurons via a specific class of autoreceptor isoform (Abe et al., 1978; Beaudet et al., 1995; Helboe and Moller, 1999). Vasopressin affects its own release from magnocellular neurons by activation of two distinct vasopressin autoreceptors (Ludwig, 1998; Gouzenes et al., 1998). Diverse evidence also supports the possibility of autoreceptors for other neuropeptide systems, including neurokinin (Catalani et al., 2004), NPY (Caberlotto et al., 2000), and μ opioid (Garzón and Pickel, 2002).

A salient parallel to the finding of PDF autoreceptors is the observation that nearly half the VIP-expressing neurons in the mammalian SCN express the VPAC2 receptor (Kalamatianos et al., 2004). VIP promotes rhythmicity and synchronization of firing rhythms by SCN neurons (Aton et al., 2005), and VPAC2 autoreceptors likely contribute to this important physiology. In the *Drosophila* circadian system, the absence of PDF leads to phase dispersion among the molecular oscillators within s-vLNs (Lin et al., 2004). Further studies are now needed to determine whether PDF autoreceptor activation facilitates or inhibits s-vLN excitability, spike activity, and subsequent PDF release, and how this action alters and synchronizes the molecular oscillator in that critical pacemaker cell group.

Both the s-vLNs and l-vLNs Respond to DH31

The neurochemistry of the fly's circadian network is largely unknown. We used the Epac1-camps expression in the vLNs to screen several candidate *Drosophila* bioactive peptides in addition to PDF and found that DH31 induced large cAMP increases in both the l-vLNs and s-vLNs. In vitro, DH31 activates PDFr (Mertens et al., 2005) and a second related GPCR DH31r (Johnson et al., 2004). The results of this screen indicate a high degree of specificity in peptide receptivity measured by this assay and implicate DH31 as a potential modulator of the neuronal clock network. In the s-vLNs, the response to DH31 appeared smaller in the absence of PDFr, although that effect did not reach the level of significance. We suggest that the complete response to DH31 by s-LNv depends on both PDFR and another receptor, presumably DH31r. In contrast, the magnitude of the DH31 response in the l-vLNs was not altered by loss of PDFr function. Compared to PDF and DH31, all the other peptides we screened had little or no effects on Epac1-camps1 FRET signals in the vLNs. This sensor therefore represents a useful and relatively rapid method to screen for transmitter or modulator effects in the living CNS. The results of our limited peptide screen suggest that increasing its scope may yield useful new information to help further these studies.

Widespread PDF Receptivity among Circadian Pacemaker Neurons

PDF signaling plays a significant role within the circadian neural circuitry of *Drosophila* (Renn et al., 1999; Blanchardon et al., 2001; Lin et al., 2004; Stoleru et al., 2004, 2005; Grima et al., 2004). To explain this action, most current hypotheses prominently feature physiological action by PDF onto many or most of the ~150 circadian pacemakers (reviewed by Taghert and Shafer, 2006). However, currently available sera for the newly identified PDFr have not unequivocally defined the sites of PDFr expression within the clock cellular network. We therefore expanded our cAMP imaging experiments to the non-PDF expressing pacemaker neurons. We found that all non-PDF expressing clock neurons tested (the fifth s-vLNs, dLNs, DN1as, DN1ps, DN2s, and DN3s) displayed measurable cAMP increases in response to PDF. Thus, our data indicate that l-vLNs, uniquely among the neuronal pacemakers tested here, display no or very small cAMP responses to PDF. Our cAMP imaging experiments are the first to directly measure physiological responses to PDF in clock neurons and present genetic

evidence consistent with the hypothesis that the effect of PDF on the s-vLNs is direct. Furthermore, given the similar magnitudes, shapes, and latencies of the PDF responses in the non-PDF-expressing clock neurons to those of the s-vLNs, we suggest that the effects of PDF on non-PDF-expressing pacemakers are also direct.

The majority of vehicle-treated clock neurons displayed a flat FRET profile with a monoexponential loss of FRET over the time courses reported here. Clear exceptions to this pattern were seen among the $DN1_p$s. Several of these neurons showed unstable FRET values, suggesting dynamic endogenous cAMP signaling. Indeed, low-frequency oscillations in FRET values were observed in several cells. Recently, Epac1-camps-based cAMP sensors have been used to investigate the mechanistic basis of spontaneous, low-frequency cAMP oscillations in an insulin-secreting cell line (Landa et al., 2005) and in the neonatal retina (Dunn et al., 2006). It is possible that similar oscillations were occurring in the $DN1_p$s. These neurons have been identified as deep brain circadian photoreceptors (Rieger et al., 2003; Veleri et al., 2003; Klarsfeld et al., 2004.) and have recently been implicated as key pacemakers in genetic backgrounds that support locomotor rhythms in constant light (Murad et al., 2007; Stoleru et al., 2007).

In summary, we have established that Epac1-camps can be used to define GPCR/cAMP signaling mechanisms within living neurons of the *Drosophila* CNS with subcellular resolution. Given the fact that the modulation of cAMP signaling is a prevalent mode of nervous system function, we anticipate that Epac1-camps will prove a useful tool for future live imaging studies in the intact, mature nervous system. Using live Epac1-camps imaging, we have established the existence of widespread, though not uniform, receptivity to PDF throughout the circadian clock network, thereby directly confirming the longstanding hypothesis that PDF is a physiological modulator of the *Drosophila* neuronal clock network.

EXPERIMENTAL PROCEDURES

Fly Rearing and Stocks

Drosophila were reared on cornmeal/agar media supplemented with yeast and kept either in a 25°C incubator or at room temperature. All Gal4 lines used in this study have been described previously: *Bmr(j)-Gal4* (Renn et al., 1999), *Pdf(m)-Gal4* (Taghert et al., 2001), *Cry(39)-Gal4* (Klarsfeld et al., 2004), *Crz*-Gal4 (Johnson et al., 2005), and *30Y-Gal4* (Zars et al., 2000. The creation of *uas-Epac1-camps(42A)* and *uas-Epac1-camps(50A)* is described below. The han^{5304} mutant was described by Hyun et al. (2005), the *uas-PDFr(16L)* by Mertens et al. (2005), and the *yw*;;*pdf-GAL80* by Stoleru et al. (2004).

Creation of *uas-Epac1-camps* Lines

BglII and an XhoI restriction sites were placed upstream and downstream respectively of full-length Epac1-camps (Nikolaev et al., 2004) by PCR amplification of Epac1-camps from its *pcDNA3* vector (Invitrogen) with a BglII site-incorporated primer 5′-ATA GGG AGA TCT AAG CTT ATG GTG AGC AAG-3′ and a XhoI site-incorporated primer 5′-ATG CTC GAG CGG CCG CTT ACT TGT AC-3′. Thermocycling reaction conditions were as follows: 30 cycles of 95°C for 60 s, 50°C for 30 s, and 68°C for 300 s. The amplified fragment was purified following agarose gel electrophoresis by the Qiaex II kit (QIAGEN) and cloned into the *pUAST* vector. The DNA was injected into w^{1118} embryos by Model Systems Genomics (Duke University). Eleven independent transgenic homozygous lines were established. Two lines, *uas-Epac1-camps(42A)* (X chromosome) and *uas-Epac1-camps(50A)* (IInd chromosome) were chosen for this study based on their support of high *Gal4*-directed Epac1-camps expression. Particular *Gal4/uas-Epac1-camps* combinations were studied as first generation cross progeny or as stable combinations created in several different genetic backgrounds.

Live Imaging

For both epifluorescent and laser confocal FRET imaging, living brains expressing Gal4-driven *uas-Epac1-camps* were dissected under ice-cold calcium-free fly saline containing 46 mM NaCl, 180 mM KCl, and 10 mM Tris (pH 7.2). Dissected brains were placed at the bottom of a 35 × 10 mm plastic FALCON Petri dish (Becton Dickenson Labware), beneath hemolymph-like saline (HL3) containing 70 mM NaCl, 5 mM KCl, 1.5 mM $CaCl_2$, 20 mM $MgCl_2$, 10 mM $NaHCO_3$, 5 mM trehalose, 115 mM sucrose, and 5 mM HEPES (pH 7.1) (Stewart et al., 1994). Brains were sufficiently adherent to the dishes to allow for time-course imaging of up to 30 min durations.

Epifluorescent microscopy was performed through a LUMPL 60×/1.10 water objective with immersion cone and correction collar (Olympus) on a Zeiss Axioplan microscope. Excitation and emission filter wheels were driven by a Lambda 10-3 optical filter changer and shutter control system (Sutter Instrument Company) and controlled with SLIDEBOOK 4.1 software (Intelligent Imaging Innovations). Emission, excitation, and dichroic filters (Chroma; sets #86002v2-SPR and -JP4) included a BA430/25 (excitation) filter, and BA470/30 and BA535/30 (emission) filters. Images were captured on a Hamamatsu Orca ER cooled CCD camera (Hamamatsu Photonics). Exposure times were 13 ms for YFP-FRET and 500 ms for CFP-donor images, as these were the shortest exposure times that allowed for clear images and yielded approximately equal ranges of values for YFP-FRET and CFP-donor emissions in untreated brains (data not shown).

Confocal images were obtained through either a XLUMPlanFI 20×/0.95 or LUMPL 60×/1.10 water objective (with immersion cones) on an Olympus FV500 confocal microscope (Olympus). Brains were scanned with a 442 nm helium-cadmium laser line. CFP-donor and YFP-FRET emissions were separated by means of a SDM515 dichroic mirror and BA480/30 and BA540/30 (center wavelength/full width half-max) emission filters.

Live FRET imaging of Epac1-camps expressing neurons was always performed on individual cells through a LUMPL 60×/1.10 water objective with immersion cone and correction collar (Olympus). For time-course experiments, brains were placed in 1.8 ml of HL3 saline in 35 × 10 mm culture dishes. We performed peptide washouts by exchanging three volumes (3 × 2000 μl) of HL3 Saline for the 2000 μl of treatment peptide. To avoid movement artifacts, we did not image neurons during washout. With the exception of our washout experiments in which we sampled every 15 s, YFP FRET and CFP donor images were captured every 5 s. For the epifluorescent microscope, YFP and CFP images were taken sequentially at each time point (by manufacturer estimate the filter-wheel switches positions within 31 ms). For the confocal microscope, YFP and CFP were scanned simultaneously onto separate photomultiplier tubes. Following 30–60 s of baseline YFP/CFP FRET measurement, 200 μl of 10× drug or peptide in 1.0% DMSO was added dropwise to the dish with a micropipette over an ~10 s period with constant image capture. The effects of applied agents on YFP-FRET and CFP-donor emissions were then observed for an additional 6 to 10 min. FSK and ddFSK were purchased from Sigma. *Drosophila* PDF and DMS were produced by Neo-MPS. DH 44, MTYamide, and vasoactive intestinal peptide were produced by Phoenix Pharmaceuticals. Allatostatin C was produced by Bachem. Pituitary adenylate cyclase-activating polypeptide 38 was purchased from Sigma. Calcitonin was kindly provided by Dr. Ian Dickerson (University of Rochester Medical Center). Small neuropeptide F was kindly provided by Dr. Peter Evans (Babraham Institute, UK). DH31 and IPNamide were kindly provided by Dr. Erik Johnson (Wake Forest University).

Data Analysis

For every region of interest (ROI), background-subtracted CFP and YFP intensities were recorded. The ratio of YFP/CFP emission was determined after subtracting CFP spillover into the YFP channel from the YFP intensity as described by Nikolaev et al. (2004). CFP spillover into the YFP channel was determined by multiplying the CFP intensity at each time point by the proportion of CFP spillover into the YFP channel—measured as 0.397 for the

epifluorescent and 0.274 for the confocal microscopes, respectively; YFP spillover into the CFP channel was negligible. Thus, for each time-point FRET was calculated by the expression

$$(\mathrm{YFP} - (\mathrm{CFP} * \mathrm{SO}^{\mathrm{CFP}}))/\mathrm{CFP}$$

where YFP and CFP are the YPF and CFP intensities from which the intensity of a background ROI has been subtracted for both channels and SO^{CFP} is the proportion of CFP spillover into the YFP channel. To compare FRET time courses across different experiments, the YFP/CFP ratio values for each neuron were subjected to smoothing by a seven-point moving average and then normalized to the value of the first time-point (=1.0). For all experiments, the effects of different manipulations were summarized as averaged plots in which the filtered and normalized values for every neuron were averaged for each time point within a given treatment. The effects of various concentrations of PDF were additionally summarized by the average maximum FRET loss displayed for each concentration (i.e., the lowest YFP-FRET/CFP-donor value on the filtered and normalized plot) expressed as the proportion of FRET lost. Untreated brains displayed a monoexponential loss of FRET caused by uneven photobleaching of YFP and CFP, a commonly observed phenomenon in FRET imaging. We did not subtract this loss of signal from any of the FRET plots of peptide- and vehicle-treated neurons. Therefore, the effects of various treatments in this report are reported relative to the loss of signal due to photobleaching observed in vehicle treated controls.

All statistical analysis was performed with Statistical Package for the Social Sciences (SPSS) version 15.0 for Windows. Single or two-factor repeated-measures ANOVAs were performed to analyze trends within time-series data. When more than two levels existed for one factor, a Tukey's honestly significant difference (HSD) post-hoc comparison was performed. For the effects of PDF concentration, single- or two-factor ANOVA was also performed on maximum FRET loss values. When more than two levels existed at one factor, a Tukey's HSD post-hoc comparison was performed. To analyze the data from washout experiments, data from cells were grouped separately into prewash and postwash groups. The prewashed group (PDF or vehicle treatment prior to washout) was analyzed through single-factor repeated-measures ANOVA followed by Tukey's HSD to determine homogenous subsets. The postwashed groups (vehicle treated, washout, and mock-washout) were treated in the same way and the homogenous subsets of treatments were compared. In both the prewash and postwash cases, the averaged FRET values were used as a response variable for a single-factor ANOVA followed by a Tukey's HSD. Tables S1–S10 present the complete statistical analysis of all observations.

Immunocytochemistry

The immunocytochemical methods used here are described in Shafer et al. (2006), as is the *pwF6-R32* line, a fly in which the clock neuron network is labeled by p element-directed β-galactosidase expression. Rabbit anti-HAN [anti-PDFr(N)] was kindly provided by Dr. Jaesob Kim (Korea Advanced Institute of Science & Technology). The rabbit anti-PDFr(C) is described in Mertens et al. (2005). Both anti-PDFr sera were used in dilutions of 1:500. Mouse anti β-galactosidase (Promega; catalog # Z3781, lot # 149211) was diluted 1:1000.

SUPPLEMENTAL DATA

The Supplemental Data for this article can be found online at http://www.neuron.org/cgi/content/full/58/2/223/DC1/.

ACKNOWLEDGMENTS

We thank Seol Hee Im, Joel Levine, Ralf Stanewsky, Ed Levitan, and Ken Blumer for comments on the manuscript. We thank Michael Nitabach, Peter Evans, Ian Dickerson, Erik Johnson, Andray Shaw, and Jaesob Kim for generously sharing reagents. We thank Jennifer Trigg, Weihua Li, and Dennis Oakley for technical assistance and Bloomington Stock Center for *Drosophila* stocks. This work was supported by an NRSA (#2F32NS053222-02) to O.T.S., by grants from the NIMH (#MH067122) and NINDS (#NS21749) to P.H.T., and by an NIH Neuroscience Blueprint Core Grant (#NS057105) to Washington University.

Received: October 2, 2007
Revised: January 22, 2008
Accepted: February 14, 2008
Published: April 23, 2008

REFERENCES

Abe, H., Kato, Y., Chihara, K., Iwasaki, Y., and Imura, H. (1978). Central effect of somatostatin on the secretion of growth hormone in the anesthetized rat. Proc. Soc. Exp. Biol. Med. *159*, 346–349.

Aton, S.J., Colwell, C.S., Harmar, A.J., Waschek, J., and Herzog, E.D. (2005). Vasoactive intestinal polypeptide mediates circadian rhythmicity and synchrony in mammalian clock neurons. Nat. Neurosci. *8*, 476–483.

Beaudet, A., Greenspun, D., Raelson, J., and Tannenbaum, G.S. (1995). Patterns of expression of SSTR1 and SSTR2 somatostatin receptor subtypes in the hypothalamus of the adult rat: relationship to neuroendocrine function. Neuroscience *65*, 551–561.

Blanchardon, E., Grima, B., Klarsfeld, A., Chélot, E., Hardin, P.E., Préat, T., and Rouyer, F. (2001). Defining the role of *Drosophila* lateral neurons in the control of circadian rhythms in motor activity and eclosion by targeted genetic ablation and PERIOD protein overexpression. Eur. J. Neurosci. *13*, 871–888.

Bos, J.L. (2003). Epac: a new cAMP target and new avenues in cAMP research. Nat. Rev. Mol. Cell Biol. *4*, 733–738.

Caberlotto, L., Fuxe, K., and Hurd, Y.L. (2000). Characterization of NPY mRNA-expressing cells in the human brain: co-localization with Y2 but not Y1 mRNA in the cerebral cortex, hippocampus, amygdala, and striatum. J. Chem. Neuroanat. *20*, 327–337.

Catalani, E., Gangitano, C., Bosco, L., and Casini, G. (2004). Expression of the neurokinin 1 receptor in the mouse retina. Neuroscience *128*, 519–530.

de Rooij, J., Zwartkruis, F.J., Verheijen, M.H., Cool, R.H., Nijman, S.M., Wittinghofer, A., and Bos, J.L. (1998). Epac is a Rap1 guanine-nucleotide-exchange factor directly activated by cyclic AMP. Nature *396*, 474–477.

de Souza, N.J., Dohadwalla, A.N., and Reden, J. (1983). Forskolin: a labdane diterpenoid with antihypertensive, positive inotropic, platelet aggregation inhibitory, and adenylate cyclase activating properties. Med. Res. Rev. *3*, 201–219.

DiPilato, L.M., Cheng, X., and Zhang, J. (2004). Fluorescent indicators of cAMP and Epac activation reveal differential dynamics of cAMP signaling within discrete subcellular compartments. Proc. Natl. Acad. Sci. USA *101*, 16513–16518.

Dunn, T.A., Wang, C.T., Colicos, M.A., Zaccolo, M., DiPilato, L.M., Zhang, J., Tsien, R.Y., and Feller, M.B. (2006). Imaging of cAMP levels and protein kinase A activity reveals that retinal waves drive oscillations in second-messenger cascades. J. Neurosci. *26*, 12807–12815.

Garzón, M., and Pickel, V.M. (2002). Ultrastructural localization of enkephalin and mu-opioid receptors in the rat ventral tegmental area. Neuroscience *114*, 461–474.

Gouzenes, L., Desarmenien, M.G., Hussy, N., Richard, P., and Moos, F.C. (1998). Vasopressin regularizes the firing pattern of rat hypothalamic neurons. J. Neurosci. *18*, 1879–1885.

Grima, B., Chélot, E., Xia, R., and Rouyer, F. (2004). Morning and evening peaks of activity rely on different clock neurons of the *Drosophila* brain. Nature *431*, 869–873.

Helboe, L., and Moller, M. (1999). Immunohistochemical localization of somatostatin receptor subtypes sst1 and sst2 in the rat retina. Invest. Ophthalmol. Vis. Sci. *40*, 2376–2382.

Helfrich-Förster, C. (1995). The period clock gene is expressed in central nervous system neurons which also produce a neuropeptide that reveals the projections of circadian pacemaker cells within the brain of *Drosophila melanogaster*. Proc. Natl. Acad. Sci. USA *92*, 612–616.

Helfrich-Förster, C. (1998). Robust circadian rhythmicity of *Drosophila melanogaster* requires the presence of lateral neurons: a brain-behavioral study of disconnected mutants. J. Comp. Physiol. [A] *182*, 435–453.

Hewes, R.S., and Taghert, P.H. (2001). Neuropeptides and neuropeptide receptors in the *Drosophila melanogaster* genome. Genome Res. *11*, 1126–1142.

Hyun, S., Lee, Y., Hong, S.T., Bang, S., Paik, D., Kang, J., Shin, J., Lee, J., Jeon, K., Hwang, S., et al. (2005). *Drosophila* GPCR Han is a receptor for the circadian clock neuropeptide PDF. Neuron *48*, 267–278.

Johnson, E.C., Bohn, L.M., Barak, L.S., Birse, R.T., Nässel, D.R., Caron, M.G., and Taghert, P.H. (2003). Identification of *Drosophila* neuropeptide receptors by G protein-coupled receptors-beta-arrestin2 interactions. J. Biol. Chem. *278*, 52172–52178.

Johnson, E.C., Bohn, L.M., and Taghert, P.H. (2004). *Drosophila CG8422* encodes a functional diuretic hormone receptor. J. Exp. Biol. *207*, 743–748.

Johnson, E.C., Shafer, O.T., Trigg, J.S., Park, J., Schooley, D.A., Dow, J.A., and Taghert, P.H. (2005). A novel diuretic hormone receptor in *Drosophila*: evidence for conservation of CGRP signaling. J. Exp. Biol. *208*, 1239–1246.

Kalamatianos, T., Kalló, I., Piggins, H.D., and Coen, C.W. (2004). Expression of *VIP* and/or *PACAP receptor* mRNA in peptide synthesizing cells within the suprachiasmatic nucleus of the rat and in its efferent target sites. J. Comp. Neurol. *475*, 19–35.

Klarsfeld, A., Malpel, S., Michard-Vanhée, C., Picot, M., Chélot, E., and Rouyer, F. (2004). Novel features of cryptochrome-mediated photoreception in the brain circadian clock of *Drosophila*. J. Neurosci. *24*, 1468–1477.

Landa, L.R., Harbeck, M., Kaihara, K., Chepurny, O., Kitiphongspattana, K., Graf, O., Nikolaev, V.O., Lohse, M.J., Holz, G.G., and Roe, M.W. (2005). Interplay of Ca^{2+} and cAMP signaling in the insulin-secreting MIN6 beta-cell line. J. Biol. Chem. *280*, 31294–31302.

Lear, B.C., Merrill, C.E., Lin, J.M., Schroeder, A., Zhang, L., and Allada, R. (2005). A G protein-coupled receptor, groom-of-PDF, is required for PDF neuron action in circadian behavior. Neuron *48*, 221–227.

Lin, Y., Stormo, G.D., and Taghert, P.H. (2004). The neuropeptide pigment-dispersing factor coordinates pacemaker interactions in the *Drosophila* circadian system. J. Neurosci. *24*, 7951–7957.

Ludwig, M. (1998). Dendritic release of vasopressin and oxytocin. J. Neuroendocrinol. *10*, 881–895.

Mertens, I., Vandingenen, A., Johnson, E.C., Shafer, O.T., Li, W., Trigg, J.S., De Loof, A., Schoofs, L., and Taghert, P.H. (2005). PDF receptor signaling in *Drosophila* contributes to both circadian and geotactic behaviors. Neuron *48*, 213–219.

Murad, A., Emery-Le, M., and Emery, P. (2007). A subset of dorsal neurons modulates circadian behavior and light responses in *Drosophila*. Neuron *53*, 689–701.

Nikolaev, V.O., and Lohse, M.J. (2006). Monitoring of cAMP synthesis and degradation in living cells. Physiology (Bethesda) *21*, 86–92.

Nikolaev, V.O., Bünemann, M., Hein, L., Hannawacker, A., and Lohse, M.J. (2004). Novel single chain cAMP sensors for receptor-induced signal propagation. J. Biol. Chem. *279*, 37215–37218.

Nikolaev, V.O., Gambaryan, S., Engelhardt, S., Walter, U., and Lohse, M.J. (2005). Real-time monitoring of the PDE2 activity of live cells: hormone-stimulated cAMP hydrolysis is faster than hormone-stimulated cAMP synthesis. J. Biol. Chem. *280*, 1716–1719.

Nikolaev, V.O., Bünemann, M., Schmitteckert, E., Lohse, M.J., and Engelhardt, S. (2006). Cyclic AMP imaging in adult cardiac myocytes reveals far-reaching β_1-adrenergic but locally confined β_2-adrenergic receptor-mediated signaling. Circ. Res. *99*, 1084–1091.

Nitabach, M.N., Blau, J., and Holmes, T.C. (2002). Electrical silencing of *Drosophila* pacemaker neurons stops the free-running circadian clock. Cell *109*, 485–495.

Nitabach, M.N., Wu, Y., Sheeba, V., Lemon, W.C., Strumbos, J., Zelensky, P.K., White, B.H., and Holmes, T.C. (2006). Electrical hyperexcitation of lateral ventral pacemaker neurons desynchronizes downstream circadian oscillators in the fly circadian circuit and induces multiple behavioral periods. J. Neurosci. *26*, 479–489.

Park, J.H., Helfrich-Förster, C., Lee, G., Liu, L., Rosbash, M., and Hall, J.C. (2000). Differential regulation of circadian pacemaker output by separate clock genes in *Drosophila*. Proc. Natl. Acad. Sci. USA *97*, 3608–3613.

Peng, Y., Stoleru, D., Levine, J.D., Hall, J.C., and Rosbash, M. (2003). *Drosophila* free-running rhythms require intercellular communication. PLoS Biol. *1*, e13. 10.1371/journal.pbio.0000013.

Picot, M., Cusumano, P., Klarsfeld, A., Ueda, R., and Rouyer, F. (2007). Light activates output from evening neurons and inhibits output from morning neurons in the *Drosophila* circadian clock. PLoS Biol. *5*, e315. 10.1371/journal.pbio.0050315.

Ponsioen, B., Zhao, J., Riedl, J., Zwartkruis, F., van der Krogt, G., Zaccolo, M., Moolenaar, W.H., Bos, J.L., and Jalink, K. (2004). Detecting cAMP-induced Epac activation by fluorescence resonance energy transfer: Epac as a novel cAMP indicator. EMBO Rep. *5*, 1176–1180.

Ponsioen, B., van Zeijl, L., Moolenaar, W.H., and Jalink, K. (2007). Direct measurement of cyclic AMP diffusion and signaling through connexin43 gap junctional channels. Exp. Cell Res. *313*, 415–423.

Renn, S.C., Park, J.H., Rosbash, M., Hall, J.C., and Taghert, P.H. (1999). A *pdf* neuropeptide gene mutation and ablation of PDF neurons each cause severe abnormalities of behavioral circadian rhythms in *Drosophila*. Cell *99*, 791–802.

Rieger, D., Stanewsky, R., and Helfrich-Förster, C. (2003). Cryptochrome, compound eyes, Hofbauer-Buchner eyelets, and ocelli play different roles in the entrainment and masking pathway of the locomotor activity rhythm in the fruit fly *Drosophila melanogaster*. J. Biol. Rhythms *18*, 377–391.

Rieger, D., Shafer, O.T., Tomioka, K., and Helfrich-Förster, C. (2006). Functional analysis of circadian pacemaker neurons in *Drosophila melanogaster*. J. Neurosci. *26*, 2531–2543.

Shafer, O.T., Helfrich-Förster, C., Renn, S.C., and Taghert, P.H. (2006). Reevaluation of *Drosophila melanogaster's* neuronal circadian pacemakers reveals new neuronal classes. J. Comp. Neurol. *498*, 180–193.

Stewart, B.A., Atwood, H.L., Renger, J.J., Wang, J., and Wu, C.F. (1994). Improved stability of *Drosophila* larval neuromuscular preparations in haemolymph-like physiological solutions. J. Comp. Physiol. [A] *175*, 179–191.

Stoleru, D., Peng, Y., Agosto, J., and Rosbash, M. (2004). Coupled oscillators control morning and evening locomotor behaviour of *Drosophila*. Nature *431*, 862–868.

Stoleru, D., Peng, Y., Nawathean, P., and Rosbash, M. (2005). A resetting signal between *Drosophila* pacemakers synchronizes morning and evening activity. Nature *438*, 238–242.

Stoleru, D., Nawathean, P., Fernández, M.de L., Menet, J.S., Ceriani, M.F., and Rosbash, M. (2007). The *Drosophila* circadian network is a seasonal timer. Cell *129*, 207–219.

Suh, G.S., Wong, A.M., Hergarden, A.C., Wang, J.W., Simon, A.F., Benzer, S., Axel, R., and Anderson, D.J. (2004). A single population of olfactory sensory neurons mediates an innate avoidance behaviour in *Drosophila*. Nature *431*, 854–859.

Taghert, P.H., and Shafer, O.T. (2006). Mechanisms of clock output in the *Drosophila* circadian pacemaker system. J. Biol. Rhythms *6*, 445–457.

Taghert, P.H., Hewes, R.S., Park, J.H., O'Brien, M.A., Han, M., and Peck, M.E. (2001). Multiple amidated neuropeptides are required for normal circadian locomotor rhythms in *Drosophila*. J. Neurosci. *21*, 6673–6686.

Veleri, S., Brandes, C., Helfrich-Förster, C., Hall, J.C., and Stanewsky, R. (2003). A self-sustaining, light-entrainable circadian oscillator in the *Drosophila* brain. Curr. Biol. *13*, 1758–1767.

Wang, J.W., Wong, A.M., Flores, J., Vosshall, L.B., and Axel, R. (2003). Two-photon calcium imaging reveals an odor-evoked map of activity in the fly brain. Cell *112*, 271–282.

Willoughby, D., and Cooper, D.M. (2006). Ca^{2+} stimulation of adenylyl cyclase generates dynamic oscillations in cyclic AMP. J. Cell Sci. *119*, 828–836.

Zars, T., Fischer, M., Schulz, R., and Heisenberg, M. (2000). Localization of a short-term memory in *Drosophila*. Science *288*, 672–675.